1973-01

Wave-Related Fluctuations in the Airflow Above Natural Waves

Davidson, Kenneth L.

Journal of Physical Oceanography, Volume 3, January 1973
http://hdl.handle.net/10945/45794

Wave-Related Fluctuations in the Airflow Above Natural Waves[1]

KENNETH L. DAVIDSON AND ALLEN J. FRANK[2]

Naval Postgraduate School, Monterey, Calif.

(Manuscript received 3 February 1972, in revised form 19 June 1972)

ABSTRACT

Simultaneous observations of wave heights and velocity fluctuations at two levels above the waves are analyzed to examine properties of the wave-related fluctuations in the airflow. Results are obtained from spectral and joint probability density function, conditional mean function (JPDF-CMF) analyses. Results are examined with respect to predictions from potential flow theory and recent theoretical formulations for wind-wave coupling. Of interest are recent formulations which allow interaction between the wave-induced motion and turbulence in the airflow, the so-called "turbulence" models.

Cospectral results exhibit features which are predicted by theoretical formulations with regard to height variations of the wave-related momentum transfer. These features include the oscillatory variations predicted by recent turbulence models and also enhanced transfer at both levels as predicted by the quasi-laminar model.

JPDF-CMF analyses are used to obtain phase-amplitude information for those variables examined in the spectral analyses. For a period in which the presence of the "critical level" could have been a factor, the phase relation between the wave-related vertical velocity and the wave height agrees with the quasi-laminar prediction. For periods in which only the turbulence in the airflow would be expected to influence the wave-induced motion, phase and amplitudes of the wave-related fluctuations differ from the potential flow predictions.

It is concluded that the interaction between the wave-induced motion and airflow turbulence had a significant effect on the observed wave-related fluctuations. Another conclusion is the assertion of the value in using JPDF-CMF analyses for examining wave-related fluctuations.

1. Introduction

Several applied geophysical problems have reached levels where improved solutions require more detailed information about energy exchanges and the structure of the near-surface layer over the ocean. These problems include, for example, surface wave predictions which utilize semi-empirical formulae requiring wind speeds at specified levels in the surface layer; and extended-period weather predictions which require, for the surface layer, specification of kinetic energy losses and thermal energy gains. Initial efforts to determine the structure and fluxes of the overwater surface layer consisted primarily of examining overwater results for the suitability of applying empirical methods which had been determined, or at least tested, in numerous overland experiments. The key assumptions in such an approach are that proper mean wind profiles can be defined, and that the waves' influence on turbulent processes in shear flow is negligible. However, as the number of overwater observations have increased, so have the number of conflicts with such strictly empirical interpretations. Perhaps the best known case is that of the drag coefficient for which there exist various representations for the dependence on wind speed.

The discrepancies among results from well-executed experiments are difficult to explain because of the lack of better dynamical descriptions of the waves' influence on the overlying airflow. Such a description is lacking due to both a late start in formulating appropriate analytical models and a scarcity of appropriate observational results. Advances in wind-wave measurements and wind-wave coupling models now appear to allow the experimentalist to compare his results with those predicted by the theoretician. This study, in part, considers such a comparison.

2. Background and approach

In August and September of 1968, measurements were made of the airflow over waves on Lake Michigan. Analyses of the data showed rather clearly that the airflow was being influenced by the underlying wave field. These data were analyzed primarily by spectral methods, and reported by Davidson (1970). Since these results were among the few which had shown such organization of airflow over natural waves (Elder *et al.*, 1970; Yefimov and Sizov, 1969), it was considered imperative that caution be used in such an interpretation of the data until further studies were available.

[1] Presented at the Conference on the Interaction of the Sea and the Atmosphere, 1–3 December, 1971, Ft. Lauderdale, Fla.

[2] Present affiliation: Squadron 3-RVAH-3, Naval Air Station, Albany, Ga.

One such study is reported here. It consists of a re-examination of the Lake Michigan data by using what appear to be more revealing analysis procedures. This study was performed during 1971. Interestingly, since 1970, several results have appeared from theoretical studies on the airflow over waves in which allowance was made for interaction between the wave-induced motion and turbulence in the airflow. These predicted results provide fortuitous independent comparisons with the results obtained in these extended analyses of the Lake Michigan data.

Theoretical formulations for wind-wave coupling have ranged from the initial quasi-laminar models (Miles, 1957), wherein the wave-induced motion interacts with the shear flow only at the "critical level,"[3] to recent formulations by Reynolds (1968), Davis (1970, 1972) and Yefimov (1970), wherein there is also interaction with the turbulent Reynolds stresses (turbulence models). It is beyond the scope of this discussion to describe or evaluate any of the approaches in the more recent turbulence models. However, such a discussion was given by Davis (1972) in which he also expressed the need for experimental data which would indicate the role of turbulence in wind-wave coupling. The objective of our study is to describe features in these data which we interpret to be due to interactions between the wave-induced motion and the turbulence in the airflow.

Part of the approach in describing these results will be to try to relate the observed results to results predicted by turbulence models, primarily Yefimov's, as well as to results predicted by potential flow theory. Unfortunately, this will not be done for particular theoretical solutions but, instead, for general classes of solutions. The data and solutions will be classified according to the expected significance of dynamics at the critical level in the observed features. Features of our results which we are able to discuss in terms of available theoretical predictions are height variations of the 1) wave-related stress, 2) amplitudes of the wave-related velocity fluctuations, and 3) phase relations between velocity fluctuations and wave height.

The specific analyses used to identify properties of the wave-related features in the airflow are considered to be as significant as the measurements and theoretical formulations in enabling the comparisons. These analyses are based on computations of joint-probability density functions and conditional mean functions. Their applications to the problem of delineating properties of organized motion in a fully turbulent regime were formulated by Holland (1968, 1973).

Several of the consequences of wind-wave coupling observed in this study have been noted in wind-wave tunnel investigations (Kendall, 1970; Chang *et al.*, 1971; Stewart, 1969; Lai and Shemdin, 1971; Karaki and Hsu, 1968). However, conclusions from comparisons between the observed and predicted results are perhaps limited with regard to extending the interpretation to the larger scale properties in the shear flow over natural waves. We view Kendall's study to be similar, both in features identified and in interpretations, to this one.

[3] Level where the mean wind speed is equal to the phase speed of the surface wave.

3. The observations

The observational data represent a selection from those described by Davidson (1970). The referenced report is available so this will be an abridged discussion on measurement and data reduction procedures. The reference also includes results from other periods, extended discussions of associated meteorological data, and additional statistics for those periods considered in this paper.

The data are from simultaneous measurements from a fixed tower of wind (u and w) and temperature fluctuations (T') and wave heights (η). The velocity and temperature measurements were made at two levels above the mean water level. Waves were measured at a point directly below the airflow sensors.

The measurements were made from a U. S. Lake Survey research tower located in 15 m of water 1.6 km from shore near Muskegon, Mich. The structure, an open triangular truss secured by a concrete anchor at each leg, was designed both to achieve stability and to minimize disturbance to the airflow and water motions.

A plumb line arrangement of sensors enabled determination of phase relations between the waves and fluctuations in the air. Sensors in the airflow and the wave gage extended westward 2.5 times the width of the tower's side. Extension arms, consisting of 5-cm rectangular tubing, were sturdy enough to avoid motion due to the airflow or waves. Also, a vertical pipe extended from below the water to 2 m above the water so the sensors could be positioned at any height from the wave crest to 2 m. Above the 2 m level, arms were located at the 4, 8 and 15 m levels.

The turbulent velocity measurements were made with constant temperature hot-wire anemometers with each probe consisting of two wires arranged in an X-configuration in order to simultaneously measure the two fluctuating wind components of interest (u and w). The probes were calibrated both *in situ*, using coincident cup and propeller anemometer measurements, and in a wind tunnel.

A high-response resistance thermometer, in a Wheatstone bridge circuit, was used to measure temperature fluctuations. The waves were measured with a capacitance gage.

Airflow sensors were oriented such that the mean wind ($\bar{U}$) was in the same plane as the two wires in the X-probe array. Therefore, the component which is designated u refers to the fluctuating component in the direction of the mean wind, determined for the measurement period. This orientation was monitored during

the measurements using a wind vane which was mounted above the probe support. Measurements were stopped if the sensor orientation and mean wind direction appeared to attain a constant difference of more than 10°.

A criterion for making measurements was that the predominant wave train, or swell, had to propagate in the direction of the mean wind. Because Lake Michigan is not so large, the presence of separate weather systems over it and hence swell propagating from different directions is not a serious problem. During the discussion of results, wind results will be presented which indicate that the wind direction at the tower was nearly the same for at least 8 hr preceding and 4 hr following each period considered. On the basis of visual observations during each period and the preceding discussion, we believe coincident directions for the mean wind and wave propagation can be assumed in the interpretations of results.

4. The analysis

Features in the fluctuating velocities were identified by both spectral analyses and joint probability density function, conditional mean function analyses which will hereafter be denoted as JPDF-CMF. Results from both analyses are used in the comparisons. The spectral estimates were obtained using the fast-Fourier transform algorithm (Cooley and Tukey, 1965). Reference should be made to Davidson (1970) for more detail on procedures used in obtaining the spectral estimates. A description follows on the JPDF-CMF analyses and methods of representing the results.

JPDF-CMF statistics were computed from normalized values of the original variables sampled at five points per second. Each record consisted of 5450 points. In order to focus the analyses on fluctuations near the frequency band corresponding to the surface waves, a bandpass filter was applied to all the data. This was performed by using a numerical inverse transform filter, which was designed on the basis of available spectral results. The response curve for the filter appears in Fig. 1 where low- and high-frequency cutoffs are shown to be approximately 0.1 and 0.8 Hz, respectively.

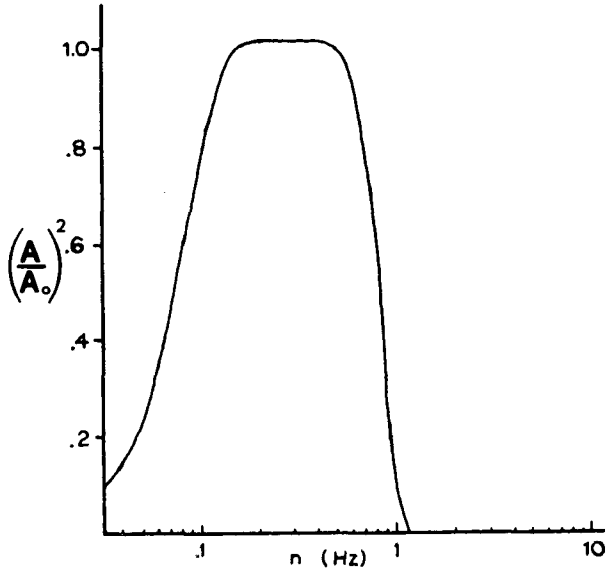

FIG. 1. Response curve $(A/A_0)^2$ for numerical inverse transform bandpass filter applied to data prior to JPDF-CMF analyses.

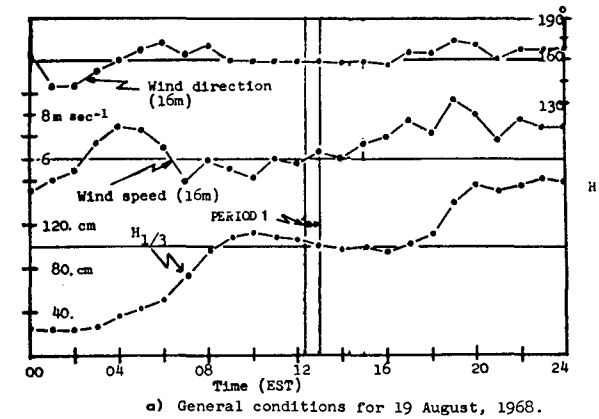

a) General conditions for 19 August, 1968.

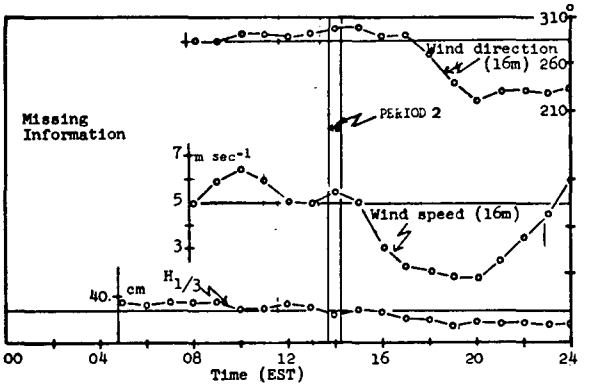

b) General conditions for 26 September, 1968.

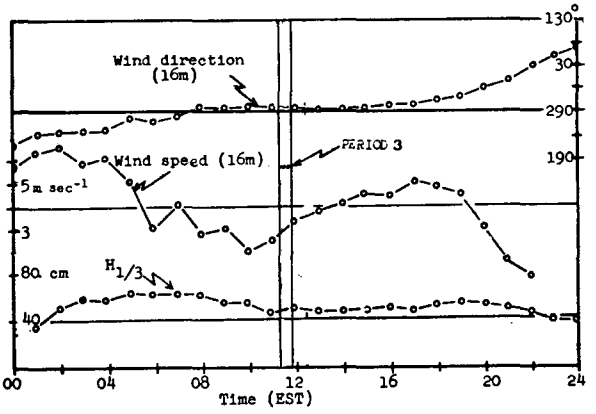

c) General conditions for 27 September, 1968.

FIG. 2. General wind and wave conditions at measurement location.

TABLE 1. General conditions for periods analyzed.

Period	Date Time (EST)	Level (m)	Wind (m sec^{-1})	Wave parameters u_*[a] (cm sec^{-1})	Ri[b]	ΔT[c] (°C)	$H_{1/3}$[d] (cm)	n_0[e] Hz	λ[f] (m)	C[f] (m sec^{-1})	z_c[g] (m)	$\left(\frac{C}{u^*}\right)$[h]
1	19 Aug. 1968 1226–1246	1.5 4.0	3.5 4.5	20.0	0.08	1.2°C	103	0.21	35	7.4	>15	37
2	26 Sept. 1968 1355–1415	1.5 4.0	4.7 5.1	16.7	−0.56	−5.4	38	0.26	23	6.0	>15	35
3	27 Sept. 1968 1120–1140	1.0 2.0	3.1 3.5	12.1	−0.55	−3.2	42	0.26	23	6.0	>15	50

[a] Friction velocity was estimated from mean wind profiles.
[b] Richardson number, $\mathrm{Ri}=g/T(\partial T/\partial Z)/(\partial \bar{U}/\partial Z)^2$, determined for layer below 8 m.
[c] Temperature at 4 m minus surface temperature.
[d] Significant wave height, $H_{\frac{1}{3}}=4\times(\sigma$ of water surface), a good estimate of average height of highest one-third waves in the record.
[e] Frequency of the wave spectrum peak.
[f] Wavelength λ and phase speed C, corresponding to wave spectrum peak n_0 computed from the dispersion relations, $c=g/2\pi n_0$ (m sec^{-1}), $\lambda=c/n_0$ (m), where $g=9.8$ m sec^{-2}.
[g] Level, determined from mean profile, where mean wind speed equals computed phase speed C. The notation >15 indicates that C was greater than the mean wind speed at the highest measurement level.
[h] Nondimensional parameter applied in recent analyses on wind-wave coupling and presented in this study for reference.

JPDF-CMF computation procedures were adopted from descriptions by Holland (1968, 1973). Applied to three variables, these procedures yield the joint probability density function (JPDF) for a pair of variables with the conditional mean of a third variable as a function (CMF) of the first two variables: for example, the probability of joint occurrences in u and w with the corresponding average wave height (η).

The resulting trivariate statistical relationship (JPDF plus CMF) can be represented by two sets of contours on a two-dimensional array. A detailed description of such a representation, after which ours was patterned, is given by Holland (1973). The axes of the array are scaled in units of standard deviations σ of the two variables defining the JPDF. Our contour analyses were performed on arrays with 324 $\frac{1}{2}\sigma$ by $\frac{1}{2}\sigma$ joint class intervals.

One set of contours on the array connects joint class intervals of equal probability of joint occurrences for the two variables defining the JPDF. The second set of contours connects joint class intervals with the same conditional mean for the third variable. The contours were constructed using an available computer algorithm on JPDF-CMF arrays wihch had previously been smoothed by a procedure described by Holland (1973). The smoother was a nine-point weighted average with weights of $\frac{1}{4}$, $\frac{1}{8}$, and $\frac{1}{16}$ at the central point, four adjacent points, and four corner points, respectively, of the centered nine-box square. Intervals in the contour analyses and possible effects of smoothing are explained within the discussion of results.

In comparisons with theoretical predictions, useful information is the statistical dependence of fluctuations in the airflow on the phase of the wave. The method selected to determine phase information was described by Holland (1973) and is based on JPDF-CMF analysis procedures. Such a method is possible because polar coordinates representing the amplitude and phase angle of a variable such as the wave height (η) can be determined from the JPDF array for the variable η and its time derivative $\dot{\eta}$. Specifically, any conditional mean function of $\dot{\eta}$ and η is a CMF of phase and amplitude of the η fluctuations because for each value of the dependent variable used in computing the CMF, the coordinates in $\dot{\eta}$, η space are determined by the amplitude of the η fluctuation occurring at that time and by the phase angle within that fluctuation. For example, the conditional mean function u ($\dot{\eta}$, η) would show the dependence of the horizontal component of wind velocity on the phase and amplitude of the waves. In this study, the phase is defined in terms of octants measured counterclockwise in the $\dot{\eta}$, η coordinate system (JPDF array) from the positive $\dot{\eta}$ axis.

Phase-amplitude information obtained in this manner offers greater latitude for our interpretations than that obtained by spectral analysis. For example, phase information determined by the JPDF-CMF procedures is not a result of linear expansions of the fluctuations and, therefore, should reflect any quasi-periodic features with frequencies higher than the dominant frequency but less than the high-frequency cutoff of the band-pass filter. In our interpretation of phase-amplitude results, we will accept Kendall's (1970, p. 279) suggestion that non-sinusoidal wave-forms are evidence of nonlinearities and, hence, a non-negligible role for turbulence. Furthermore, spectral analyses yield phase information as a function of frequency only. In a JPDF-CMF approach, as will be seen, phase relations can be examined according to wave amplitude classes. These aspects of the phase-amplitude results from the JPDF-CMF analysis along with convenient methods for representing the relationships are presented during the discussion of results.

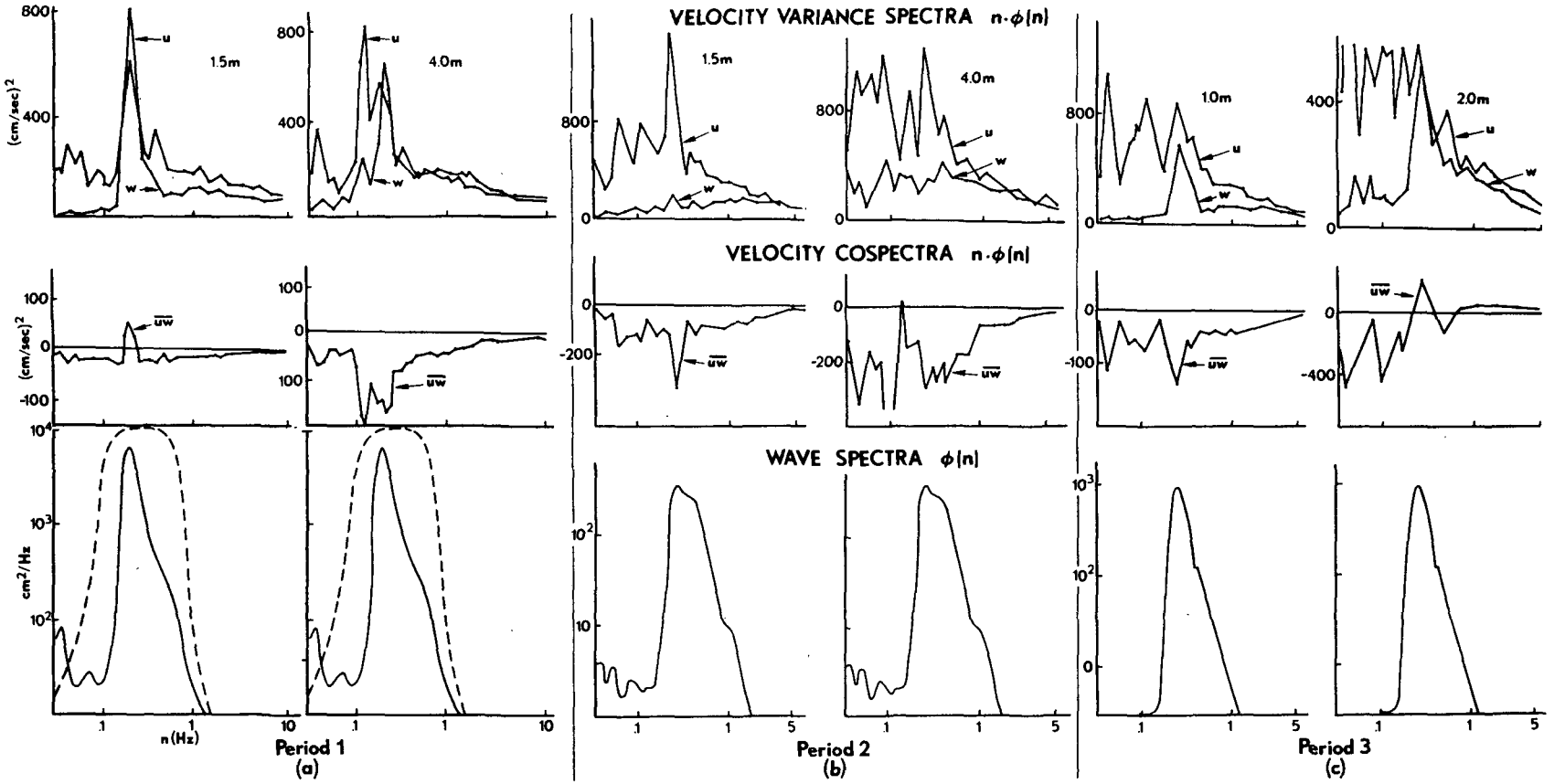

FIG. 3. Velocity variance and covariance spectra and wave spectra (bandpass filter superimposed for (a) period 1 (19 August, 1226–1246 EST) 1.5 and 4.0 m levels indicated; (b) period 2 (26 September, 1355–1415 EST) 1.5 and 4.0 m levels indicated; (c) period 3 (27 September, 1120–1140 EST) 1.0 and 2.0 m levels indicated.

5. Results

The results are from observational periods of 20-min duration on three separate days, 19 August, and 26 and 27 September, 1968. These periods will be denoted as period 1, 2 and 3, respectively, in the following discussions. They were selected for this study because previous spectral analyses on these data revealed significant wave-related fluctuations and more important, perhaps, revealed features similar to those obtained in numerical solutions (Davis, 1970; Yefimov, 1970).

General meteorological and wave conditions encompassing these periods appear in Fig. 2 and in Table 1. General conditions could be described as being steady, certainly not representing active wave growth or rapid decay. Of the three periods, period 2 has the highest mean wind speeds, and, although the critical level is indicated in Table 1 as being above 15 m, the dynamics of the critical level will be considered as being important for this period. Winds were low relative to the wave phase speed during periods 1 and 3 so features in the airflow for these periods should reflect those due primarily to the interaction between the wave-induced motion and turbulence in the airflow. The latter situation, although not of much interest for wave generation problems, is representative of conditions over most of the oceans when swell propagates into regions of relatively light winds. As such, the results are relevant to describing the surface layer over the ocean. Fig. 2 also depicts the steady wind directions prior to the periods.

Velocity variance and covariance spectra and wave variance spectra for the three periods appear in Fig. 3 where each panel corresponds to one of the periods. Velocity spectra for lower and upper levels appear on the left- and right-hand sides of each panel, respectively, and wave spectra appear on both sides. In this format, coincident extrema in wave and velocity spectra can be readily identified. Velocity spectra are represented as $n\phi_{uw}(n)$ vs $\ln n$ so the area under the curve is proportional to the contribution to the variance or covariance from a frequency band.

Smoothing was applied to the original spectral estimates for this presentation. Original spectra, consisting of 16,384 spectral values, were reduced to 128 spectral values by averaging over neighboring values. The number of values averaged together increased logarithmically with frequency, and near the frequency of the wave spectra peaks was approximately ten. The procedure has been described by Oort and Taylor (1969) and yields final spectra wherein averaged spectral values are evenly spaced when plotted on a logarithmic scale. Also, minor fluctuations were removed in preparation of Fig. 3. The band-pass filter applied to all data after the spectral analyses but prior to the JPDF-CMF analyses appears as a dashed line superimposed on the wave spectra in panel (a).

The presence of wave-related velocity fluctuations during these observations is indicated by the coincident

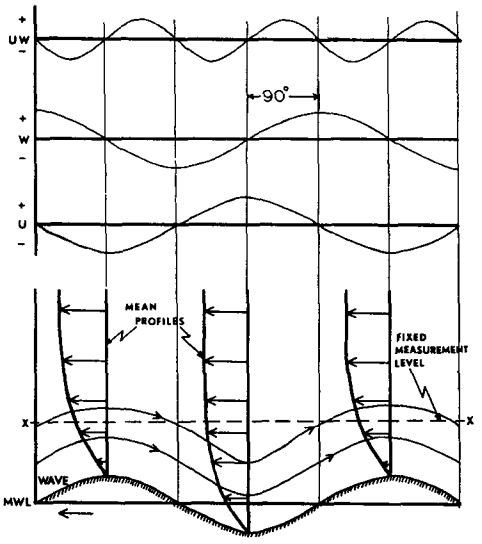

FIG. 4. Potential flow predictions for velocity fluctuations observed from a fixed sensor over progressive wave.

peaks in the velocity, u and w, and wave variance spectra for all periods. These coincident peaks, however, are not sufficient evidence of interaction between the wave-induced motion and the shear flow as predicted in the theoretical formulations. Because the velocity measurements were made at fixed levels above the mean water level, airflow streamline bending by the waves could have produced these spectral features. Because this possibility has to be considered in our interpretations, potential flow predictions for a shear flow above a progressive wave are shown in Fig. 4.

The extrema in the co-spectra, $\overline{uw}$, near the frequency of the wave spectra peaks in Fig. 3, are indicative of wind-wave coupling. The extrema, in fact, represent both enhanced and decreased momentum transfer, $-\overline{uw}$, due to the wave-related motion. As seen from Fig. 4, these features are not predicted by potential flow theory because in this case u and w are in quadrature. Enhanced momentum transfer similar to that seen in Fig. 3 is predicted by the quasi-laminar formulations due to the dynamics at the critical level. An oscillatory vertical variation of the wave-related momentum transfer is predicted by turbulence models (Yefimov, 1970; Reynolds, 1968).

We observe that enhanced momentum transfer occurred at both levels during period 2 (Fig. 3, panel b) which had the largest wind speeds; hence, dynamics at the critical level could have been a factor. We also observe that oscillatory variation in the momentum transfer occurred during periods 1 and 3 (Fig. 3, panels a and c) when dynamics at the critical level were, perhaps, of little significance. We will not try to interpret the opposing wave-related oscillations be-

tween periods 1 and 3[4]; however, Yefimov (1970, his Figs. 2 and 4) obtained both types of height variations in his solutions.

The oscillatory appearance for the wave-related momentum transfer is a significant, if not startling, result of these observational data. As such, it has to be interpreted cautiously. The feature was observed in laboratory experiments by Stewart (1969) and Kendall (1970). Stewart (1970), in fact, viewed his results as being too sensitive to measurement errors to make comparisons with theoretical predictions. Results from tests of probe alignment effects and the shape of the spectra away from the dominant wave frequency lead us to believe that the observed oscillations are accurate representations of the airflow.

Although spectral results have revealed some features appearing in recent turbulence models, further interpretations on the basis of spectral results have, perhaps, been discredited. This is because the interpretations of these results implicate the importance of nonlinear processes whose properties are not necessarily revealed by spectral analysis. Therefore, further comparisons and interpretations will be made from JPDF-CMF analyses.

JPDF-CMF results for u, w and η (waves) appear in Fig. 5. Each panel again corresponds to a specific period and all results for a level appear on one side of the panel. The notation indicates which variables define the JPDF and for which variable the conditional mean was computed. For example, η (u, w) indicates that u and w define the JPDF and that the conditional mean was computed for η.

The formats of all JPDF-CMF results are the same. The abscissa and ordinate for all arrays extend from -4σ to $+4\sigma$. Contours defining the JPDF are those for the 0.5%, 2.5%, and higher (in 2.5% increments) per sigma-squared probability levels. Contours defining the CMF are those for the $\pm 1.5\sigma$, $\pm 1.0\sigma$, $\pm 0.5\sigma$ and 0 conditional mean values of the third variable. Comparisons of smoothed results with unsmoothed results revealed that the effect of smoothing on the primary features was negligible. The main features were certainly easier to delineate after the smoother was applied.

Contours for the JPDF's and CMF's can be distinguished by the closed concentric patterns for the JPDF's. The zero CMF contour appears as a dashed line separating regions of positive and negative values. The number in the upper right hand corner of each panel, for example $R=-0.12$, is the correlation coefficient for the two variables defining the JPDF, being proportional to the asymmetry of the JPDF contours.

[4] The sign of w at 2 m for this period has been reversed from that in the previous description (Davidson, 1970). This change also reversed the sign, positive to negative, of the wave-induced stress at that level. Discrepancies which arose with the previous representation had led to the level being described as "anomalous." Phase results from this re-examination along with results from a parallel study on microthermals have led to the decision that the previous sign for w at this level was wrong.

Although results in Fig. 5 represent probabilities of joint occurrences of fluctuations of various magnitudes in u and w in conjunction with an average surface elevation, they can also be viewed as representing physical processes. We can consider the quadrants, counterclockwise from the positive u axis, to represent

a. Quadrant 1—upward transport of positive momentum
b. Quadrant 2—upward transport of deficit momentum
c. Quadrant 3—downward transport of deficit momentum
d. Quadrant 4—downward transport of positive momentum

General patterns of $\eta(u,w)$ in Fig. 5 agree with cospectral results with respect to momentum transfer in the spectral band associated with the surface waves. These are asymmetrical orientations in JPDF's along the $+135°$ axis for levels with enhanced stress and circular, or negligible uw correlation, for levels with decreased stress. In regard to predominant processes, the levels with decreased stress do not show significant upward transfer of positive momentum, which might be expected if the positive cospectral extrema were in fact due to wave-imparted momentum. Rather, the transfer of deficit momentum, up and down, appears to be significant, especially at low probability levels beyond 5%.

Interpretation of these JPDF-CMF patterns for the physical processes and for the waves influence is easier if they are examined in conjunction with phase-amplitude results. JPDF-CMF arrays containing phase-amplitude information for u, w and uw with respect to the waves appear in Figs. 6–8. The phase-amplitude information, summarized by octants and wave amplitude classes, is also depicted in Figs. 9–11.

Procedures used to obtain these summaries were described by Holland (1973). Octants are measured counterclockwise from the positive $\dot{\eta}$ axis. Results summarized inside and outside a 1.5σ delineation, outlined in panels (a) of Figs. 6–8, are viewed in our analyses as small and large waves, respectively. This summarized result was defined by Holland as "the amplitude-stratified, weighted-phase conditional mean function." Because of the nearly concentric property of the JPDF $(\dot{\eta}, \eta)$ contours, the segments delineating octants appear to be nearly the same length. The smooth curves were drawn through the midparts of the segments.

Associated with each variable in Figs. 9–11 is a parameter τ_0. This parameter is defined as the "statistical eddy period" and is determined by the ratio

$$\tau_0 = 2\pi\sigma/\dot{\sigma},$$

where σ and $\dot{\sigma}$ are standard deviations of the variable and its derivative. A test on the appropriateness of the analysis is to compare τ_0's for the dependent variable

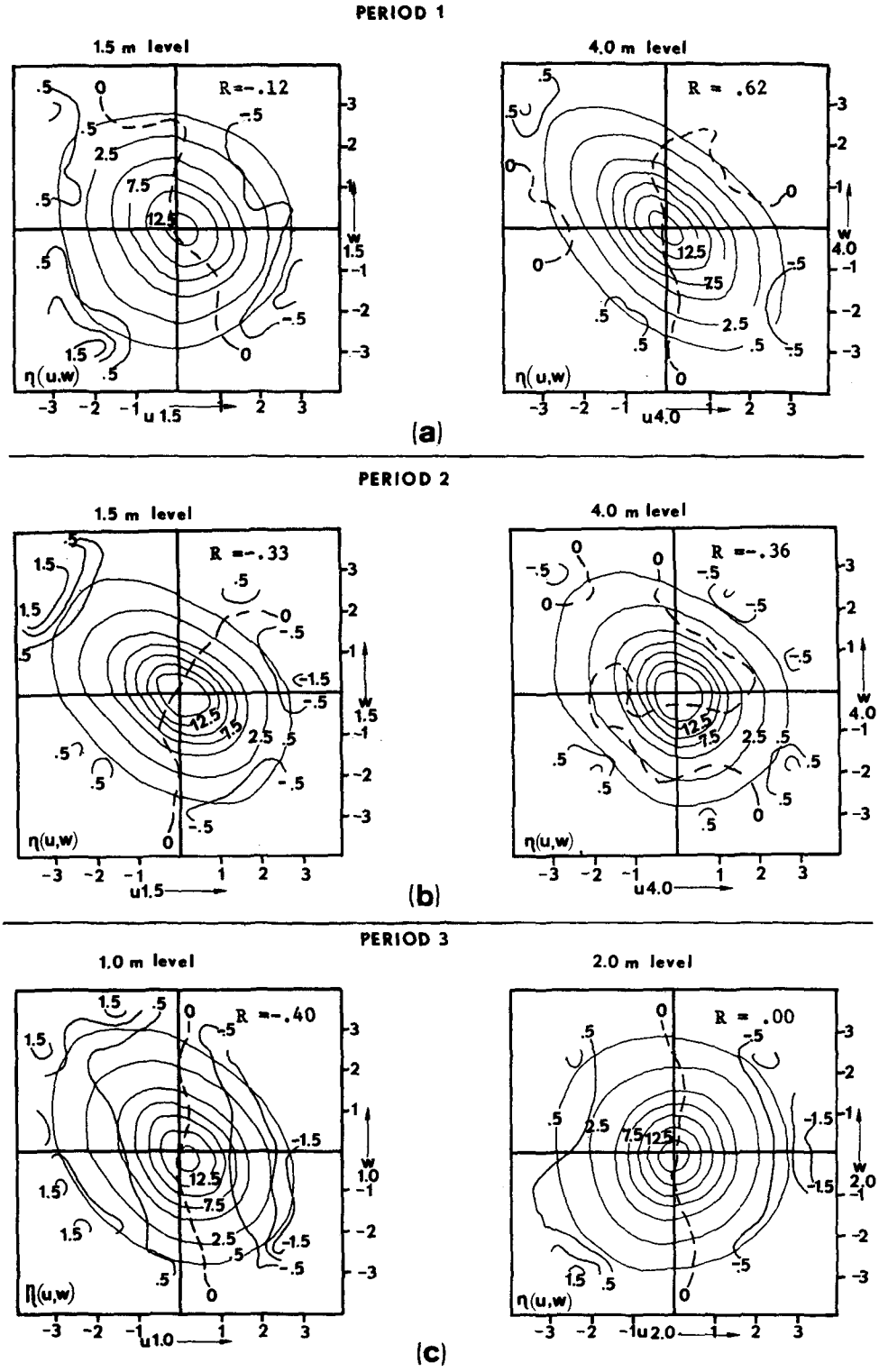

FIG. 5. (u,w,η) JPDF-CMF results for (a) period 1 (1.5 and 4.0 m levels), (b) period 2 (1.5 and 4.0 m levels), and (c) period 3 (1.0 and 2.0 m levels). Results appear on left- and right-hand sides, respectively.

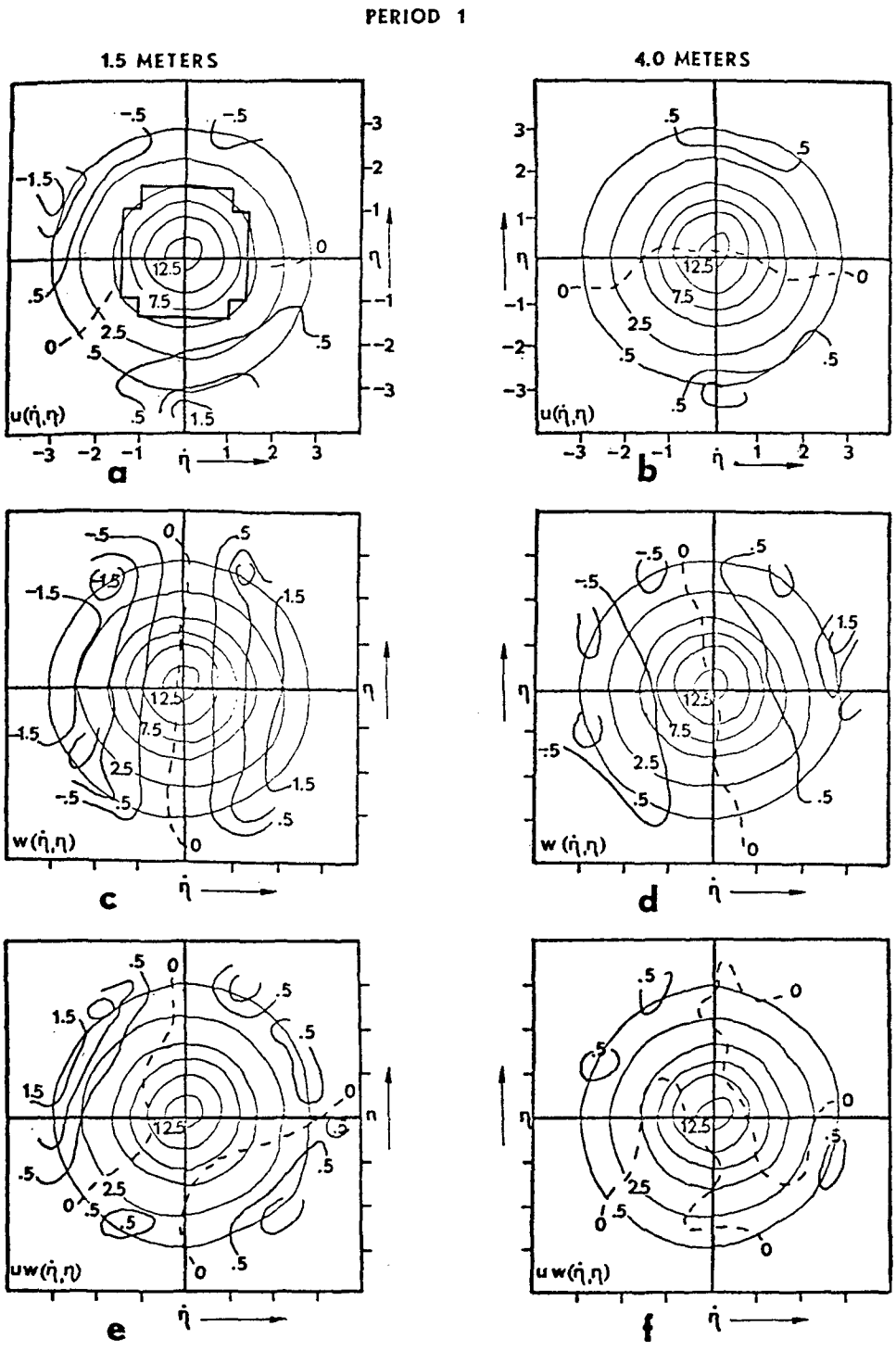

FIG. 6. $(\dot{\eta},\eta;\, u,w,uw)$ JPDF-CMF results for period 1 with 1.5 and 4.0 m level results on left- and right-hand sides. Results are basis for phase-amplitude analyses using the wave height as reference variable.

(u, w, etc.) with that for the reference variable η. Fortunately, τ_0's for the velocities are surprisingly close to those for the waves except, perhaps, those for the u component in period 2. As expected, τ_0 for the product uw is less than that for the wave because uw in a linear system, at least, would appear as a second harmonic as in Fig. 4.

Some features are noted in Figs. 9–11. First, the phase relations between the dependent variables and the waves do not shift as a function of the wave ampli-

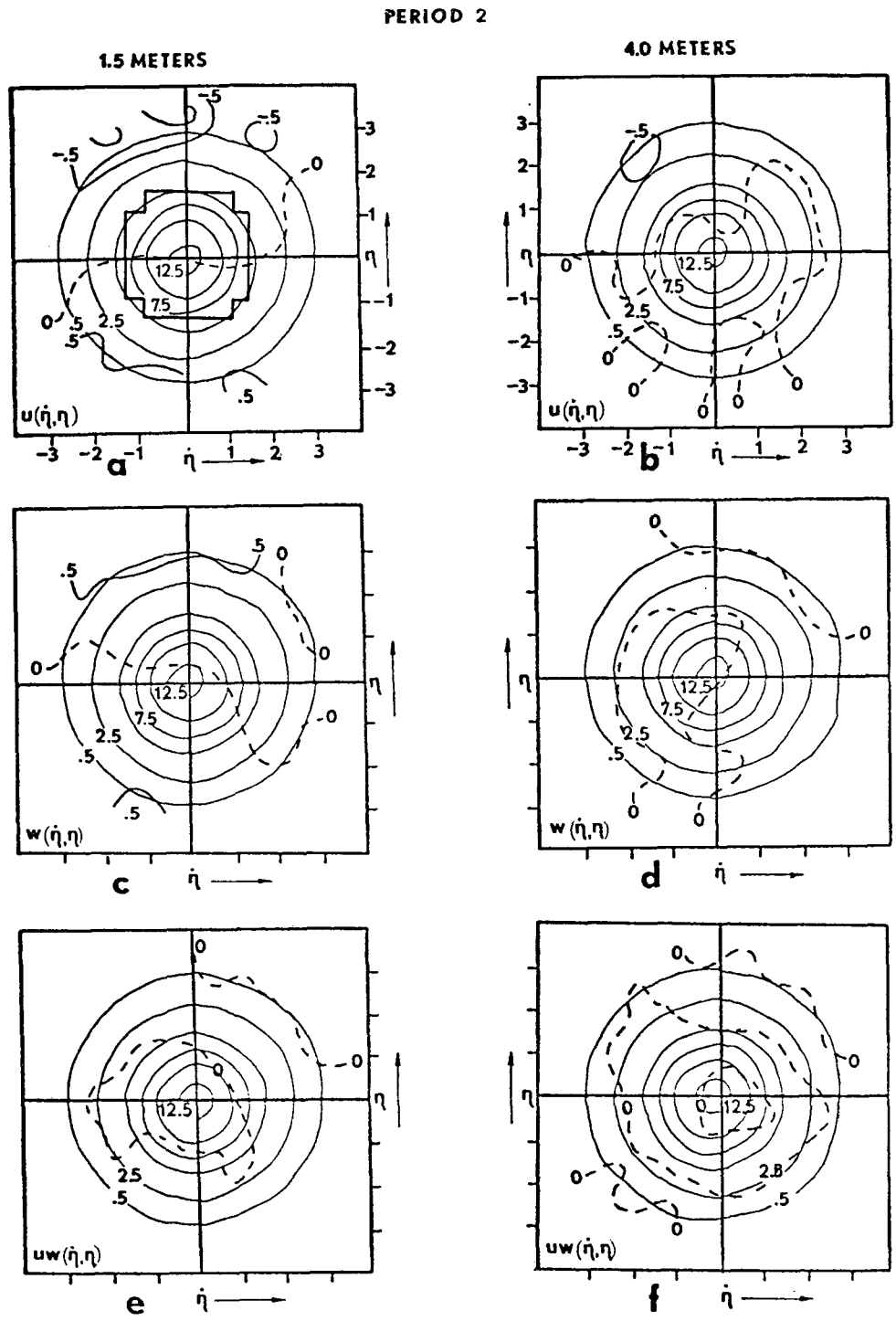

FIG. 7. Same as Fig. 6 except for period 2 at 1.5 and 4.0 m levels.

tude class. Second, the amplitudes of the dependent variables appear to change in a linear fashion with changes in wave amplitudes. Finally, the extrema in the *uw* trace are not symmetrical but instead those related to deficit momentum transfer are about twice as large as those related to positive momentum transfer. The latter feature was observed indirectly in the preliminary discussion of Fig. 5. It was also observed by Kendall (1970) in waveforms of *uw*.

Although the first two features above are not unexpected, their occurrence in these results indicate that the analyses yield results which are sensitive and con-

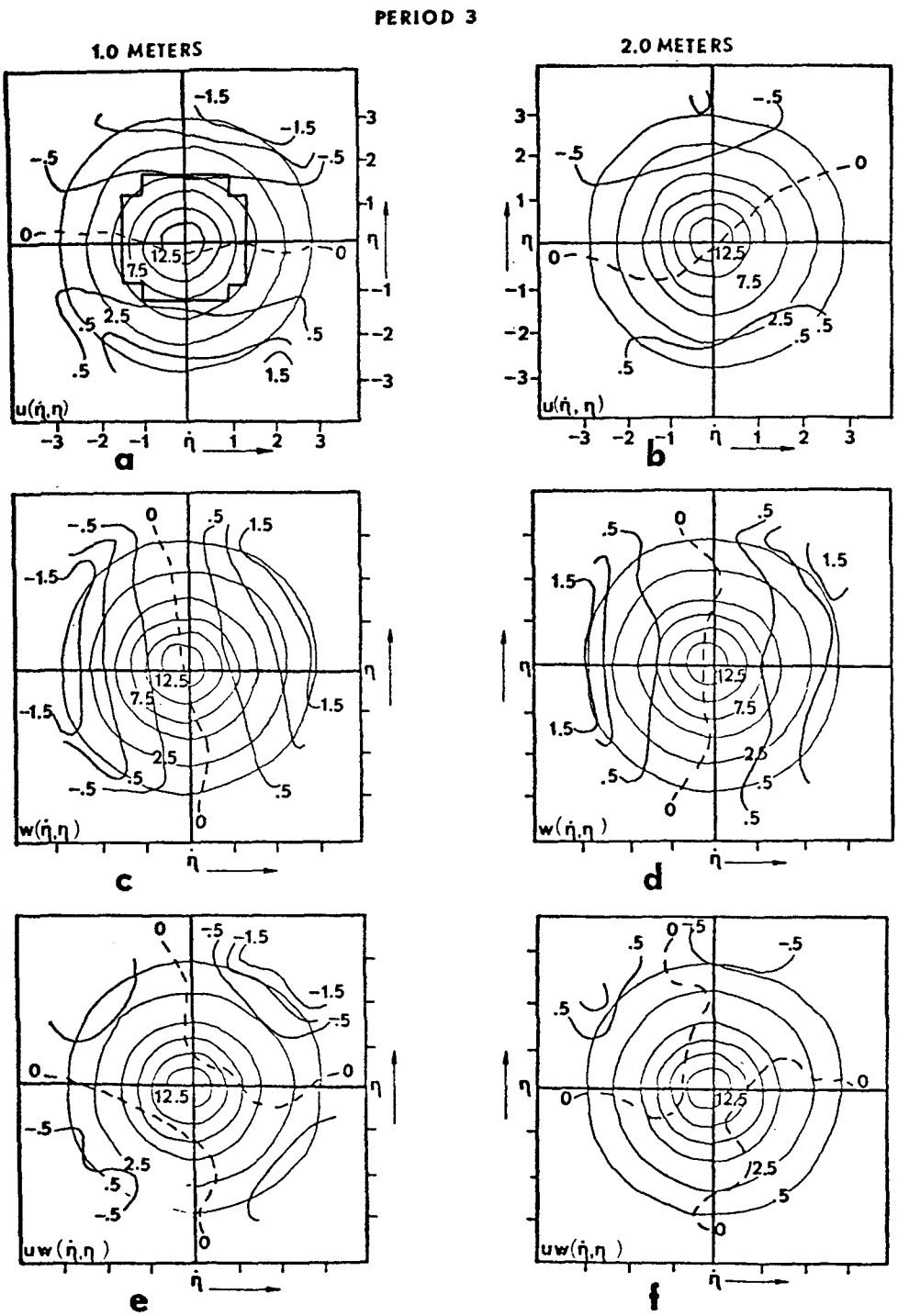

FIG. 8. Same as Fig. 6 except for period 3 at 1.0 and 2.0 m levels.

sistent with respect to mean phase and amplitude properties of the fluctuations. Furthermore, the similarity between amplitude classes allows us to focus on the large wave phase-amplitude results which are reproduced in Fig. 12, from which we will examine features of the height variations of amplitudes and phase differences. Using Fig. 12 as a reference, we will also reconsider patterns in both sets of the JPDF-CMF results.

A general description of phase-amplitude results in Fig. 12 would be that they resemble the potential flow prediction (Fig. 4) with the exception of u and w at

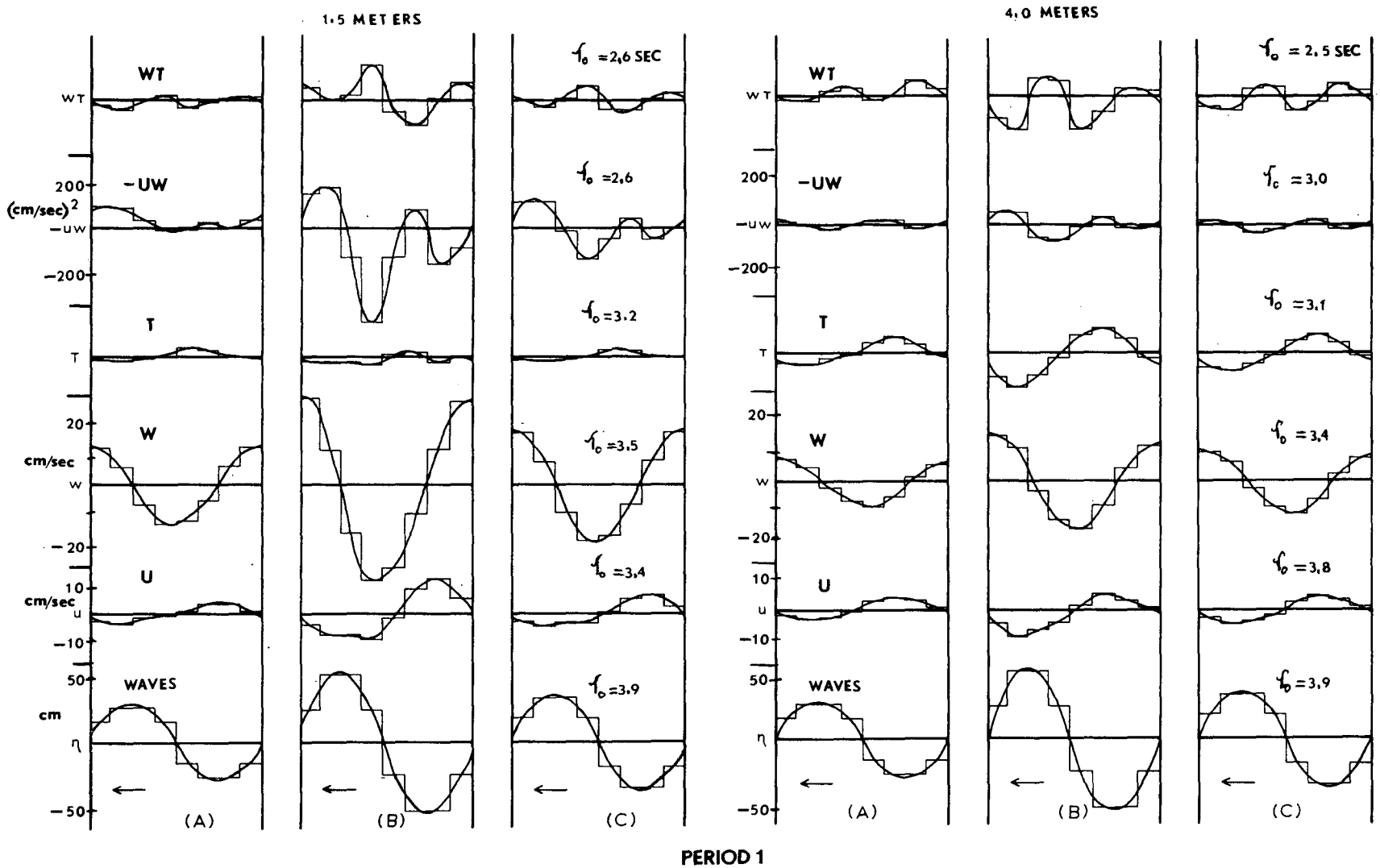

FIG. 9. Phase-amplitude results (amplitude stratified phase, weighted phase conditional mean functions) for period 1 and for indicated levels. These are summaries of results in Fig. 6. Wave propagation direction is to the left.

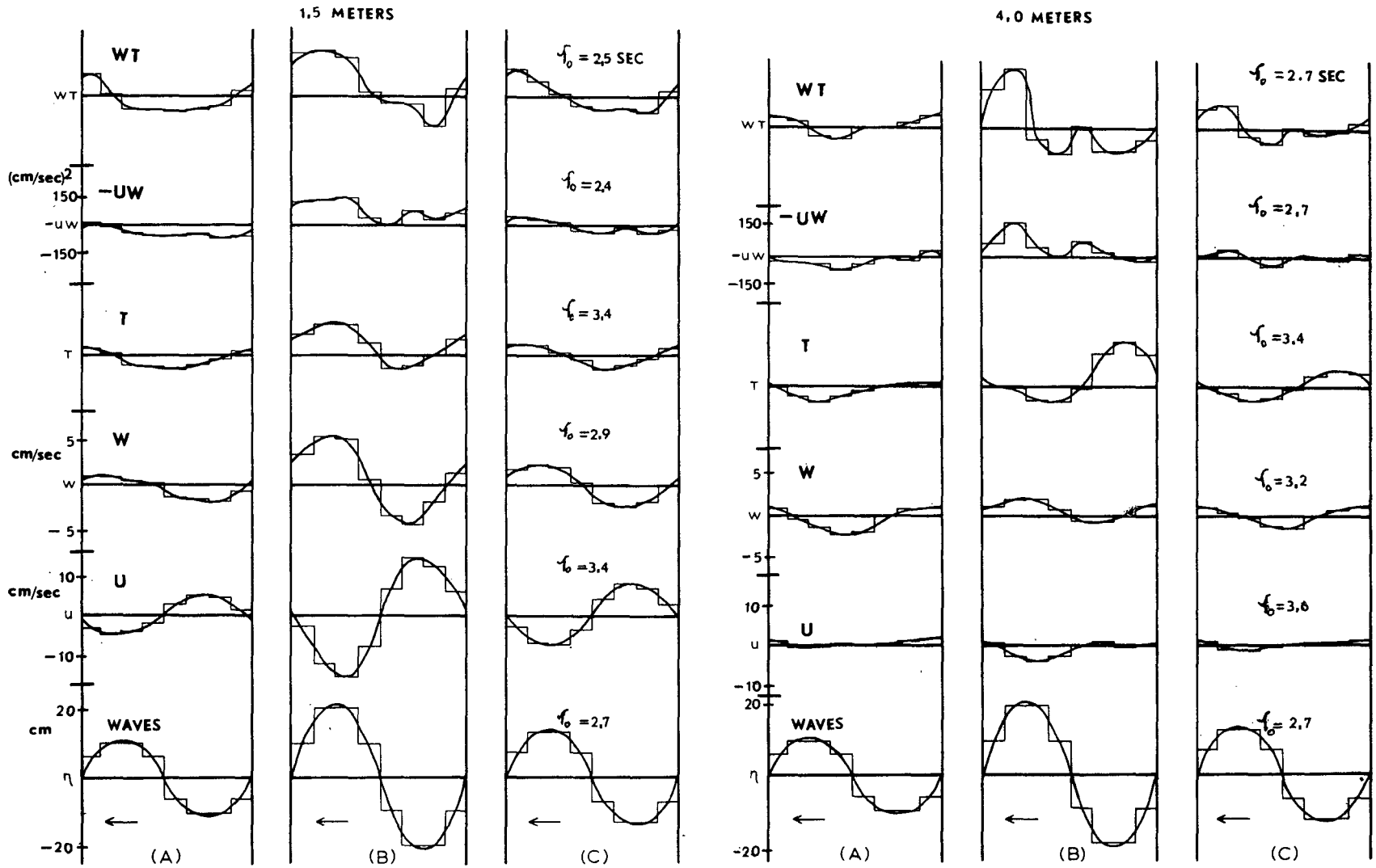

PERIOD 2

(A) SMALL WAVES (B) LARGE WAVES (C) ALL WAVES

FIG. 10. Same as Fig. 9 except for period 2. These are summaries of results in Fig. 7.

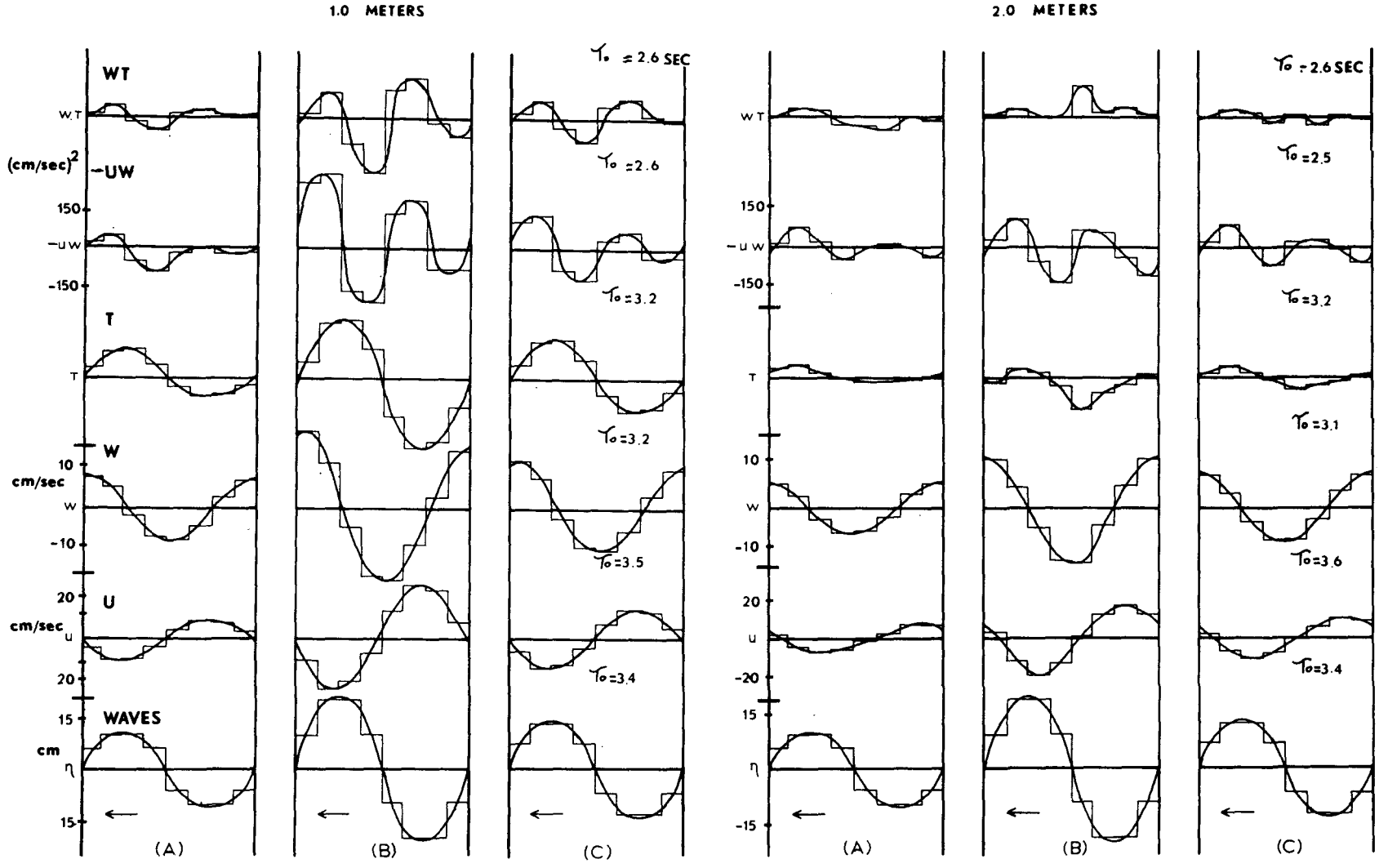

PERIOD 3

(A) SMALL WAVES (B) LARGE WAVES (C) ALL WAVES

FIG. 11. Same as Fig. 9 except for period 3. These are summaries of results in Fig. 8.

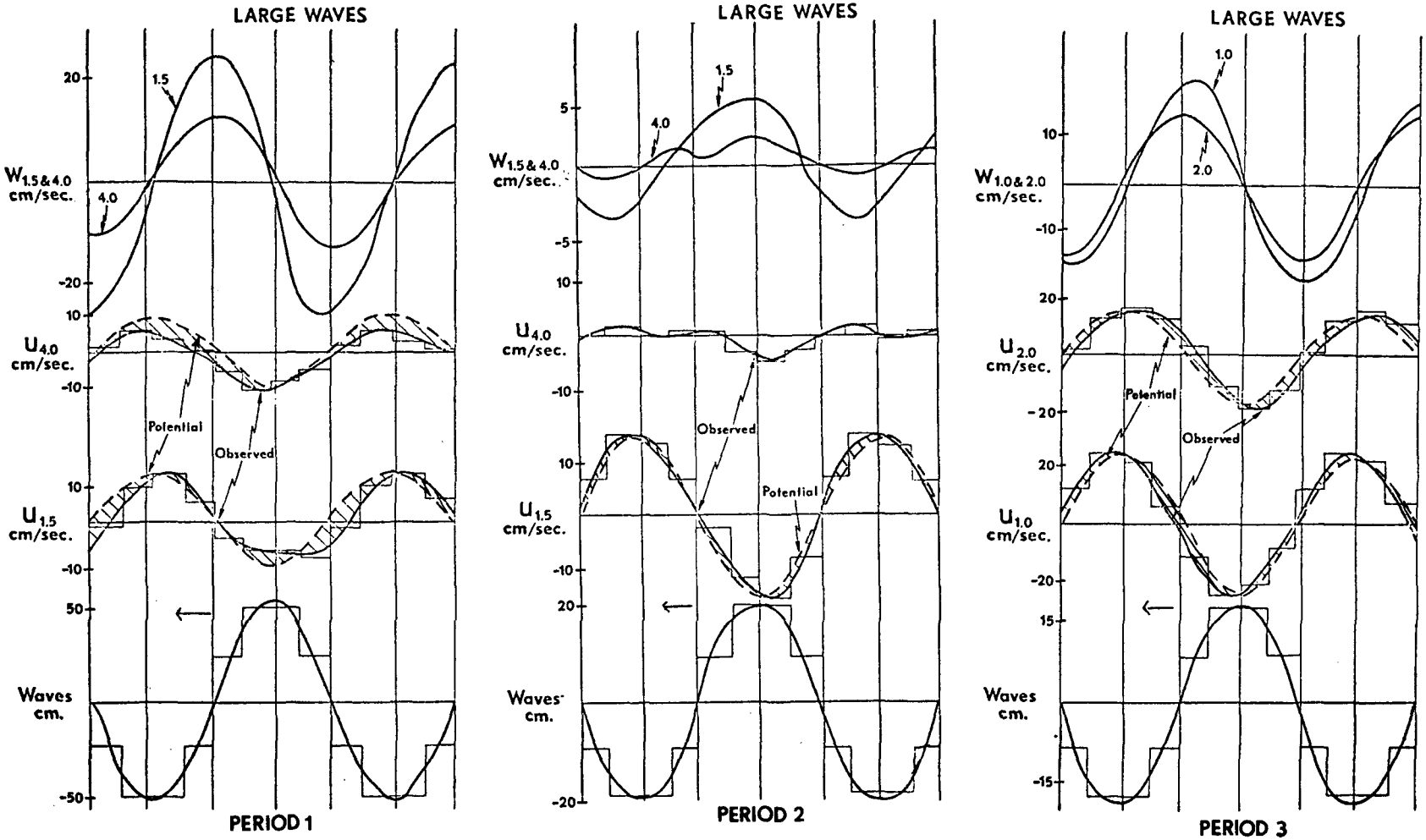

FIG. 12. Phase-amplitude results for large waves abstracted from Figs. 9–11. Dashed line represents phase, but not amplitude, predicted by potential flow theory. Wave propagation direction is to the left.

TABLE 2. Comparison of height variation of velocity amplitudes: observed vs potential predictions* in terms of the ratios between upper and lower levels.

Period	Date	u(upper)/u(lower) Observed	u(upper)/u(lower) Predicted	w(upper)/w(lower) Observed	w(upper)/w(lower) Predicted
1	19 August	0.75	0.48	0.50	0.35
3	27 September	0.70	0.36	0.67	0.18

* Determined from the formulae, $u = [ka(\bar{U}-c) - a\partial\bar{U}/\partial Z]e^{-kz}$, $w = ka(\bar{U}-c)e^{-kz}$, where $k = 2\pi/\lambda$, λ is the wavelength, a the amplitude, $\bar{U}$ the mean wind, and c the wave phase speed.

4.0 m and w at 1.5 m in period 2. Table 2 contains the results of a comparison of the height variations of the amplitudes for periods 1 and 3 with the potential flow predictions, which indicate that the decrease with height of the amplitude is less than predicted. This feature was observed in numerical results obtained by both Yefimov (1970) and Davis (1970).

Phase relationships between the velocities and waves in Fig. 12 will now be examined. We observe the following general features, which will be verified further from JPDF-CMF results.

1. For periods 1 and 3, when dynamics at the critical level were not considered to be a factor:

1a. The w component has the phase relation with the wave predicted by potential flow theory.
2a. The u component shifted back at levels where the wave-related momentum transfer is negative (1.5 m in period 1 and 2.0 m in period 3) and shifted ahead at levels where it is positive (4.0 m in period 1 and 1.0 m in period 3).

2. For period 2 when dynamics at the critical level could have been a factor:

2a. The phase of w component (at 1.5 m) shifted from the downwind mode toward the crest, as described by Phillips (1966, p. 91).
2b. The positive extrema in u (at 1.5 m) shifted forward, toward the back slope of the wave, and the negative extrema shifted back.

The phase relations just noted are, perhaps, more apparent from examinations of the JPDF-CMF patterns in Figs. 6–8 from which the above summaries were obtained. In order to facilitate such an examination, we will reference JPDF-CMF patterns which would arise if potential flow theory accurately described the observations. These patterns appear in Fig. 13.

Phase shifts in the u component were a significant aspect of the preceding results and can be re-examined by comparing CMF patterns in panels (a) and (b) of Figs. 8–10 with the pattern in Fig. 13a. Forward and backward shifts, as noted in Fig. 12, would appear as clockwise and counterclockwise rotations from the orientation of the CMF patterns in Fig. 13a. We observe that such rotations are most evident for those levels (Figs. 6a and 8b) which had negative wave-related momentum transfer and also for the level (Fig. 7a) which we believe was influenced by processes occurring at the critical level. Also, the asymmetry of the pattern rotations, particularly below the 2.5% probability level, reaffirms the existence of the non-sinusoidal waveforms in Fig. 12.

The phase shift of the w component at 1.5 m in period 2 is also evident from a comparison of the CMF pattern orientations in Figs. 7c and 13b. Interestingly, CMF patterns for other levels, represented in Figs. 6d and 8c, which had positive wave-related momentum transfer have similar, but smaller, rotations. We note that the latter shifts, which are quite apparent in the CMF patterns, are barely discernible in Fig. 12.

With regard to the observed phase results, the only result which we could readily relate to theoretical predictions was the phase of the w component at 1.5 m in period 2. The observed shift for this component is a prediction in the quasi-laminar theory and is due to critical level dynamics. The forward shift of the positive extrema in the u component at this level is also a prediction of this theory. However, the latter shift is only evident below the 2.5% probability level in Fig. 7a. The influence of the critical level could not be assumed for periods 1 and 3, however. Rather, we suggest

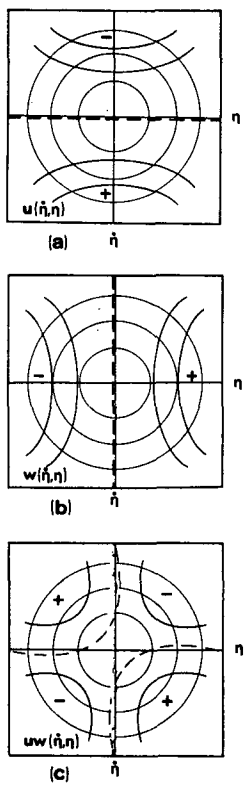

FIG. 13. Schematic of JPDF-CMF patterns which would occur if wave-related fluctuations reflected, primarily, streamline bending (potential flow). Panels correspond to those appearing in Figs. 6–8.

that the waves' influence on the airflow turbulence was the reason for the observed departures from potential flow predictions.

The latter interpretation is supported by the fact that features were observed for the wave-related momentum transfer during periods 1 and 3 which have been predicted by "turbulence" formulations for wind-wave coupling (Yefimov, 1970). Unfortunately, it has been observed[5] that phase-relation results in the latter models are very sensitive to the choice of defining parameters in the solutions. Therefore, we will not relate these results to results from particular theoretical predictions.

Finally, we view a significant aspect of these results to be the similar phase shifts which occurred at levels in periods 1 and 3 which had the same sign for the wave-related momentum transfer. If these results are representative of the influence of turbulence on the wave-related fluctuations, the results could be used in the verifications of turbulence models. The representativeness of the results, of course, would not be established on the basis of this small sample. Rather, these similarities should be examined in future analyses of these kind of data.

6. Summary and conclusions

We considered the need for better descriptions of the waves' influence on the adjacent airflow and referenced recent theoretical formulations which attempt to describe this influence. Our objective was to obtain a description of features in velocity data obtained over waves which could be interpreted with respect to the role of turbulence in wind-wave coupling. Our approach was to relate, if possible, the observed results to predictions from theoretical models.

Spectral results from three periods revealed the presence of wave-related velocity fluctuations and wave-related momentum transfer in the airflow. Observed height variations for the latter were related to predictions from recent turbulence models (e.g., Yefimov, 1970) and from the quasi-laminar model. Enhanced momentum transfer occurred at both levels in a period (period 2) when a critical level influence was possible, and oscillatory height variations occurred in the wave-related momentum transfer during two periods (periods 1 and 3) when a critical level influence was not expected.

JPDF-CMF results yielded information on non-potential features of the wave-related fluctuations. Deviations from potential flow predictions were assumed to be indicators of interaction between the wave-induced motion and the shear flow. The transfer of deficit momentum was observed to be the significant process at those levels which had negative wave-related momentum transfer. In periods 1 and 3, when the critical level was not expected to influence the results, the amplitude and phase relations of the wave-related velocity fluctuations differed from the potential flow predictions. The phase differences, although consisting of small phase shifts, were quite evident in the JPDF-CMF results. The observed shifts were similar at levels which had the same sign for the wave-related momentum transfer. In period 2, when the critical level influence was possible, the phase of the w and, possibly, the u components was observed to agree with the quasi-laminar predictions.

In conclusion, we believe that wave-related features in the velocity fluctuations and momentum transfer have been readily identified and that these features reflect the dynamic interactions between the wave-induced motion and the turbulent shear flow. These interactions are being approximated in recent theoretical formulations for wind-wave coupling. During periods 1 and 3, the observed features reflected the interaction between the wave-induced motion and the turbulence in the airflow. During period 2, the observed features agreed with those predicted as consequences of the critical level influence. The fact that the features, which were observed in data from the complex natural regime, were so readily identified and consistent encourages the use of wind-wave coupling models in describing the overwater surface layer. Such models should include the provisions for turbulence interaction.

Furthermore, JPDF-CMF analyses, as described by Holland (1968), appear to be extremely well suited for examining the airflow over waves. Our interpretations from these analyses represent only a small part of those which could have been made.

Acknowledgments. The authors wish to thank Dr. D. J. Portman, Mr. Edward Ryznar and Mr. Allen Davis for assistance in obtaining these data, and Mr. Floyd Elder and Mr. H. K. Soo for providing the complementary mean profile data. The research tower was furnished and maintained by the U. S. Army Corps of Engineers, Lake Survey Division. The research was supported by the Office of Naval Research under Contract N00014-67-A-0181-0005 with the University of Michigan and Task NR 083-265 with the Naval Postgraduate School. Numerical calculations were performed by computer facilities at the University of Michigan and the Naval Postgraduate School. The manuscript was typed by Miss Marion Marks.

[5] Information provided by R. E. Davis, Scripps Institution of Oceanography, in private communication.

REFERENCES

Chang, D. C., E. J. Plate and G. M. Hidy, 1971: Turbulent airflow over the dominant component of wind-generated water waves. *J. Fluid Mech.*, **47**, 183–208.

Cooley, J. W., and J. W. Tukey, 1965: Algorithm for the machine calculations of complex Fourier series. *Math. Comput.*, **19**, 297–301.

Davidson, K. L., 1970: An investigation of the influence of water waves on the adjacent airflow. ORA Rept. 08849-2-T, Dept. of Meteorology and Oceanography, University of Michigan, 259 pp.

Davis, R. E., 1970: On the turbulent flow over a wavy boundary. *J. Fluid Mech.*, **42**, 721–732.

——, 1972: On prediction of the turbulent flow over a wavy boundary. *J. Fluid Mech.*, **52**, 287–306.

Elder, F. C., D. L. Harris and A. Taylor, 1970: Some evidence of organized flow over natural waves. *Boundary Layer Meteor.*, **1**, 80–87.

Holland, J. Z., 1968: An application of some statistical techniques to the study of eddy structure. TID-24585, U. S. Atomic Energy Commission, Washington, D. C., 378 pp.

——, 1973. A statistical method for analyzing wave shapes and phase relationships of fluctuating geophysical variables. *J. Phys. Oceanogr.*, **3**, 139–155.

Karaki, S., and E. Y. Hsu, 1968: An experimental investigation of the structure of a turbulent wind over water waves. Tech. Rept. 68, Dept. of Civil Engineering, Stanford University, 100 pp.

Kendall, J. M., 1970: The turbulent boundary layer over a wall with progressive surface waves. *J. Fluid Mech.*, **41**, 259–282.

Lai, R. J., and O. H. Shemdin, 1971: Laboratory investigations of air-turbulence above simple water waves. *J. Geophys. Res.*, **76**, 7334–7350.

Miles, J. W., 1957: On the generation of surface waves by shear flows. *J. Fluid Mech.*, **3**, 185–204.

Oort, A. H., and A. Taylor, 1969: On the kinetic energy spectrum near the ground. *Mon. Wea. Rev.*, **97**, 623–636.

Phillips, O. M., 1966: *The Dynamics of the Upper Oceans.* Cambridge University Press, 261 pp.

Reynolds, W. C., 1968: The mechanics of an organized wave in a turbulent shear flow. Unpublished manuscript, Dept. of Mechanical Engineering, Stanford University, 39 pp.

Stewart, R. H. 1969: Laboratory studies of the velocity field over deep water waves. Ph.D. dissertation, Dept. of Oceanography, University of California, San Diego, 161 pp.

——, 1970: Laboratory studies of the velocity field of deep water waves. *J. Fluid Mech.*, **42**, 733–754.

Yefimov, V. V., 1970: On the structure of the wind velocity field in the atmospheric near-water layer and the transfer of wind energy to sea waves. *Izv. Atmos. Oceanic Phys.*, **6**, 1043–1058.

——, and A. A. Sizov, 1969: Experimental study of the field of wind velocity over waves. *Izv. Atmos. Oceanic Phys.*, **5**, 530–537.